Effect of Concrete Overlay Debonding on Pavement Performance

THOMAS VAN DAM, ELEANOR BLACKMON, AND M. Y. SHAHIN

The objectives of this paper were to determine the effect of bond loss on response and performance of bonded concrete overlays and to examine present bonding techniques and bond loss detection methodologies. A finite-element model called ILLI-SLAB was used to evaluate pavement response to load, and Westergaard-Bradbury equations were used to determine curling stresses. It was found that loss of bond adversely affects maximum pavement tensile stress (thus fatigue life) and maximum pavement deflections. It is also believed that curling stresses may cause unbonded thin overlays to separate from the underlying slab, causing extremely high stress in the overlay if a load is applied. The only way bond can be obtained is to follow good construction techniques. A summary of these techniques is presented in the paper. On the basis of the deflection analysis it was concluded that it may be possible to detect bond loss using nondestructive testing of corner deflections.

The objective of this study, sponsored by the Federal Aviation Administration, was to determine the effect of bond loss on the structural behavior and future performance of a pavement. Recommended bonding methodologies and techniques for detection of delamination in bonded concrete overlays were also addressed.

In the last 25 years, the gross weights of aircraft have increased significantly, leading to increased stress in many pavements. Many airports have experienced significant changes from light to heavy aircraft or increases in traffic volume, or both. Fully bonded portland cement concrete (PCC) overlays are often used to increase an existing pavement's load-carrying capacity. A fully bonded overlay adds directly to the pavement's load-carrying capacity by creating a monolithic pavement structure.

This study addressed the effect of commercial aircraft loading on sections with bonded PCC overlays, a type of section that may occur at airports that have experienced growth. To this end a relatively thin (for airports) 8-in. slab was assumed with bonded overlays of 3, 6, or 9 in. Unbonded overlays with the same thicknesses were also examined to model the effect of debonding. A Boeing 727 was used for the loading analysis because it usually provides the most critical commercial aircraft loading.

Bonded overlays have been used on many projects (*1-4*) with varied results. When failure occurred, it was usually attributed to loss of bond at the pavement-overlay interface. Studies have shown (*4, 5*) that loss of bond is common to some degree in almost all bonded concrete overlays; but when a substantial loss of bond occurs, the slab no longer acts as a monolithic structure, thus reducing the structural capacity of the pavement.

U.S. Army Construction Engineering Research Laboratory, P.O. Box 4005, Champaign, Ill. 61820-1305.

APPROACH

To determine the effect bond loss has on the structural behavior of overlaid concrete pavements, stresses due to loading and temperature curling were examined. This study used two different slab sizes: a 12.5- × 15.0-ft slab and a 20.0- × 20.0-ft slab. The load was applied by a Boeing 727 aircraft with a gross weight of 170,000 lb, tire pressure of 168 psi, and a tire imprint area assumed to be 12 × 20 in. It was assumed that the original pavement had a thickness of 8 in., and the PCC overlay thickness was 3, 6, or 9 in. Two different subgrade modulus of reaction values (*K*-values of 200 and 500 pci) were used and the slabs were modeled with a load transfer efficiency (LTE) of 25 percent (stress unloaded side/stress loaded side = 0.25). The procedure was repeated for the unbonded case. The load was applied at two different locations on the slab to produce maximum tensile stress and deflection. Maximum tensile stress in the concrete slab was obtained through an edge loading condition at the center of the longitudinal joint. Maximum pavement deflection occurred when the load was applied at the corner of the slab.

To determine stresses due to loading, the pavement section was analyzed using a finite-element model called ILLI-SLAB. Developed at the University of Illinois in 1977, ILLI-SLAB uses the classical theory of a medium-thick plate on a Winkler foundation (*6*). This model can analyze one- or two-layer concrete pavements with joints or cracks, and it allows for different load transfer values. The model can also analyze a bonded or unbonded condition at the layer interface.

Concrete slabs are also subjected to stresses due to the temperature gradients through the slabs. These stresses, known as curling stresses, can be high enough to cause failure (*7-9*). During the day, positive temperature gradients (surface is hotter than the bottom) that form across the slab may be as great as 3°F/in. At night, when the bottom of the slab is warmer than the surface, a gradient of -1.5°F/in. can be obtained (*7, 8*). Westergaard (*10*) derived a set of equations for estimating the magnitude of the curling stresses at the interior and edge of a slab. Bradbury (*11*) developed coefficients to easily solve the Westergaard equations. The

Westergaard-Bradbury method for analyzing curling stresses was used in this study. Curling-stress equations have also been developed by Darter (*8*). Both equations were developed for monolithic sections and are probably not valid when examining sections with unbonded overlays that act independently from the underlying slab. For this reason, the more basic equation (Westergaard-Bradbury) was used for this attempt to model the curling stresses in overlays.

The most critical stresses developed through curling are due to the positive temperature gradient that occurs when the temperature of the top of the pavement is higher than that of the bottom. This positive temperature gradient produces tensile stresses in the bottom of the slab. Stresses due to an applied load will add to the curling stresses, producing a much more critical stress level. This phenomenon has been investigated by a number of researchers (*8-10*). In this study, the edge-curling stress was predicted for each slab by the Westergaard-Bradbury equation, and the curling stress was directly added to the load-induced maximum tensile stress to estimate the total maximum tensile stress for the slab.

This approach can only be applied for bonded concrete overlays, because when bond has been lost, the overlay and existing slab act independently. Two different approaches were used to analyze the unbonded case. The first approach was to treat the unbonded overlay as if it were a lone slab sitting on an extremely stiff subgrade and to use the Westergaard-Bradbury equation to determine the edge-curling stress in the overlay. This curling stress was then added to the stress due to loading in order to determine the total maximum tensile stress in the overlay.

The second approach assumed that the overlay had curled up off the underlying slab. When such separation of the overlay and the underlying slab occurs, the overlay will experience no support. Thus an applied load will create extremely high stresses in the overlay. The ILLI-SLAB finite-element model was used to examine two cases in which part of an overlay experienced no support. The two cases simulated areas of nonsupport at corner and interior positions (Figure 1). The aircraft load was placed over the area of nonsupport and the resulting stresses were determined.

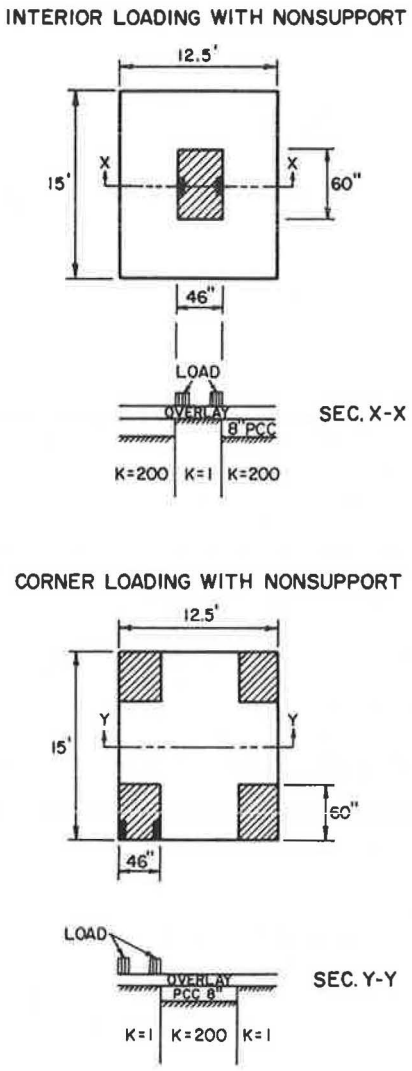

FIGURE 1 Boeing 727 interior and corner loading over areas of nonsupport.

ANALYSIS

The comprehensive analysis was performed assuming a Boeing 727 load. The maximum tensile stress and the maximum deflection induced by the applied load were determined using ILLI-SLAB. Curling stresses were determined using the Westergaard-Bradbury equations and ILLI-SLAB. The results of slab behavior due to load and temperature gradients are presented in the following subsections.

Loading Stresses

The maximum tensile stress occurs in the composite slab when it is subjected to edge loading along its longitudinal joint. A summary of stresses caused by a Boeing 727 loading is given in Table 1. The results are presented graphically in Figures 2-4. Figure 2 shows the maximum tensile stresses generated in the 12.5- × 15.0-ft slab for three overlay thicknesses and two different moduli of subgrade reaction. Figure 3 shows the same results for the 20.0- × 20.0-ft slab, and Figure 4 shows a comparison of the two slab sizes for modulus of subgrade reaction K = 200 pci.

From Figures 2 and 3, it can be observed that the maximum tensile stress in the slab is reduced by one-half when the overlay thickness is increased from 3 to 9 in. It is also evident that a stiffer subbase-subgrade leads to slightly lower maximum tensile stresses. As seen in Figure 4, when stresses in the 12.5- × 15.0-ft slab are compared with those in the 20.0- × 20.0-ft slab, little difference is noted. Thus slab size, at least within the range of the two slabs studied, has little influence on the resulting maximum tensile stresses caused by load.

Of primary interest is that loss of bond leads to a large increase in the maximum tensile stress in the slabs. It should be noted that the maximum tensile stress always occurs in the underlying slab except when the overlay is unbonded. When a bonded condition exists, the neutral axis is at the center of the

TABLE 1 MAXIMUM TENSILE STRESSES AND PAVEMENT LIFE FOR EDGE-LOADING CONDITION

Slab Size (ft)	Overlay Thickness (in.)	K (pci)	Overlay Bond	Stress (psi)	Pavement Life Coverages
12.5 × 15.0	3	200	Bonded	787	106
12.5 × 15.0	6	200	Bonded	547	777
12.5 × 15.0	9	200	Bonded	401	8,363
12.5 × 15.0	3	200	Unbonded	1,142	26
12.5 × 15.0	6	200	Unbonded	890	63
12.5 × 15.0	9	200	Unbonded	652[a]	272
12.5 × 15.0	3	500	Bonded	641	298
12.5 × 15.0	6	500	Bonded	466	2,416
12.5 × 15.0	9	500	Bonded	350	30,602
12.5 × 15.0	3	500	Unbonded	900	60
12.5 × 15.0	6	500	Unbonded	717	165
12.5 × 15.0	9	500	Unbonded	536[a]	888
20.0 × 20.0	3	200	Bonded	788	106
20.0 × 20.0	6	200	Bonded	588	493
20.0 × 20.0	9	200	Bonded	416	6,067
20.0 × 20.0	3	200	Unbonded	1,136	26
20.0 × 20.0	6	200	Unbonded	887	64
20.0 × 20.0	9	200	Unbonded	654[a]	867
20.0 × 20.0	3	500	Bonded	638	306
20.0 × 20.0	6	500	Bonded	465	2,456
20.0 × 20.0	9	500	Bonded	357	25,054
20.0 × 20.0	3	500	Unbonded	899	60
20.0 × 20.0	6	500	Unbonded	715	168
20.0 × 20.0	9	500	Unbonded	538[a]	867

[a]Maximum tensile stress in overlay.

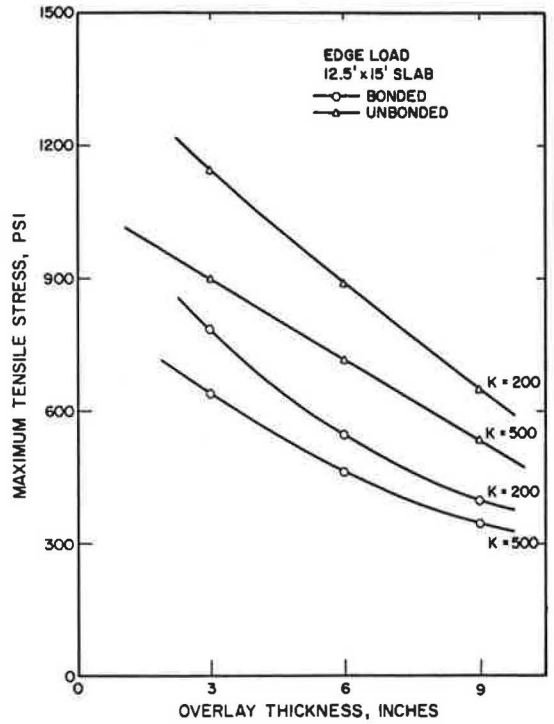

FIGURE 2 Effect of bonded and unbonded overlay thickness on tensile stress in 12.5- × 15.0-ft slab.

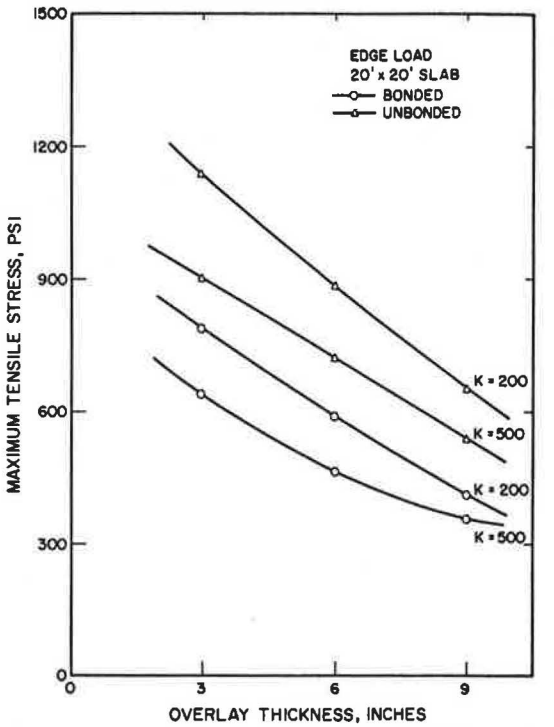

FIGURE 3 Effect of bonded and unbonded overlay thickness on tensile stress in 20.0- × 20.0-ft slab.

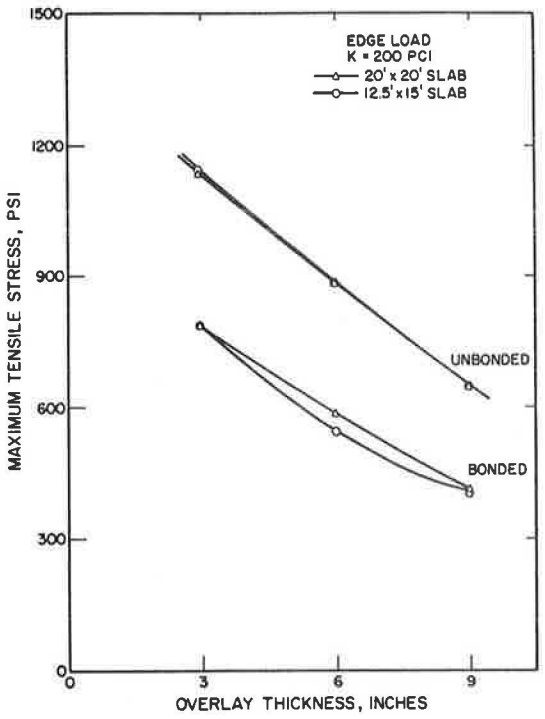

FIGURE 4 Effect of bonded and unbonded overlay thickness on slabs with subgrade K = 200 pci; stress for unbonded slabs is identical for both slab sizes.

composite slab; thus the stress at the top will have the same magnitude as that at the bottom, opposite only in direction (i.e., compression at top and tension at bottom, Figures 5 and 6). When fully bonded, the overlay will never experience tensile forces unless it is thicker than the underlying slab, and even then the tensile stresses will be quite small in comparison with the tensile forces generated in the bottom of the existing slab. For the unbonded case, each layer has a neutral axis placed at its center (Figures 5 and 6). The only time that more tensile stress could build up in the overlay than in the existing slab is when the overlay has a thicker section than the existing pavement. Table 2 gives the maximum tensile stresses that occur in the overlay for both the bonded and the unbonded condition.

The effect of these tensile stresses on pavement life was also analyzed. The modulus of rupture of the concrete was estimated using the following relationship developed by ERES Consultants (*12*):

$$MR = 209(E)^{0.736} \quad (1)$$

where E is the modulus of the concrete in millions of pounds per square inch.

For an E-value of 5 million psi, the MR was calculated to be 683 psi. When the modulus of rupture had been determined, a second equation, also developed by ERES Consultants (*12*), was used to estimate the number of applied stress repetitions (coverages) required to cause 50 percent cracking of the slabs. The Federal Aviation Administration defines one coverage as occurring when "each point in the pavement within the limits of the traffic lane has experienced a maximum stress, assuming the stress is equal under the full tire print" (*13*). A Boeing 727 has a pass (departure) to coverage ratio of 3.48. The ERES equation is as follows:

$$\text{Log (coverages)} = 2.27(MR/STRESS) + 0.056 \quad (2)$$

where

Log (coverages) = the number of coverages to 50 percent slab cracking,
MR = the third-point modulus of rupture calculated from the dynamic modulus of elasticity, and
$STRESS$ = the critical stress in the slab resulting from ILLI-SLAB.

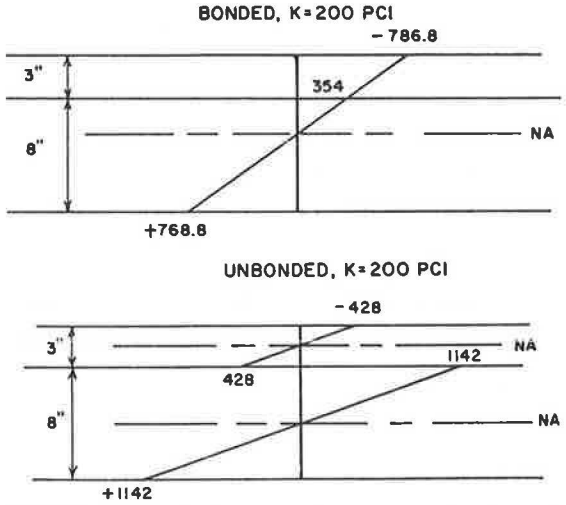

FIGURE 5 Neutral axes and maximum tensile and compressive stresses for bonded and unbonded 3-in. overlays.

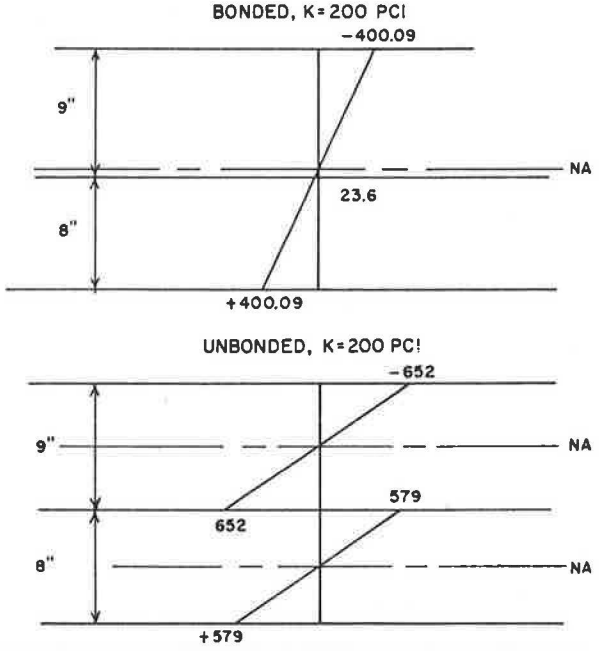

FIGURE 6 Neutral axes and maximum tensile and compressive stresses for bonded and unbonded 9-in. overlays.

TABLE 2 MAXIMUM TENSILE STRESSES CALCULATED IN THE OVERLAY FOR EDGE-LOADING CONDITION

Slab Size (ft.)	Overlay Thickness (in.)	K (pci)	Overlay Bond	Tensile Stress in Overlay (psi)
12.5 × 15.0	3	200	Bonded	-
12.5 × 15.0	6	200	Bonded	-
12.5 × 15.0	9	200	Bonded	23.6
12.5 × 15.0	3	200	Unbonded	428
12.5 × 15.0	6	200	Unbonded	668
12.5 × 15.0	9	200	Unbonded	652
12.5 × 15.0	3	500	Bonded	-
12.5 × 15.0	6	500	Bonded	-
12.5 × 15.0	9	500	Bonded	20.6
12.5 × 15.0	3	500	Unbonded	338
12.5 × 15.0	6	500	Unbonded	538
12.5 × 15.0	9	500	Unbonded	536
20.0 × 20.0	3	200	Bonded	-
20.0 × 20.0	6	200	Bonded	-
20.0 × 20.0	9	200	Bonded	24.5
20.0 × 20.0	3	200	Unbonded	426
20.0 × 20.0	6	200	Unbonded	665
20.0 × 20.0	9	200	Unbonded	654
20.0 × 20.0	3	500	Bonded	-
20.0 × 20.0	6	500	Bonded	-
20.0 × 20.0	9	500	Bonded	21.0
20.0 × 20.0	3	500	Unbonded	337
20.0 × 20.0	6	500	Unbonded	536
20.0 × 20.0	9	500	Unbonded	538

NOTE: Dashes indicate never in tension.

The resulting relationship between stress and coverages is shown in Figure 7. As can be seen, even relatively small increases in critical pavement tensile stress can lead to quite large decreases in pavement life. Using this relationship, the predicted pavement life for each slab condition was calculated (Table 1).

The following observations can be made:

1. Slab size, within the range of the two slab sizes studied, will not significantly alter predicted pavement life. A 9-in.-thick overlay bonded to a 20.0- × 20.0-ft. slab that rests on a subgrade with K = 500 pci is predicted to withstand 25,054 coverages whereas a similar bonded overlay on a 12.5- × 15.0-ft slab will withstand 30,602 coverages. As the overlays become thinner, the difference in the two predicted pavement lives becomes quite small.

2. Increasing the modulus of subgrade reaction will increase the number of coverages. For a 9-in. bonded overlay on a 20.0- × 20.0-ft slab and a subgrade K = 500 pci, a total of more than 25,000 coverages can be expected. If the subgrade stiffness is decreased to 200 pci, only 6,067 coverages are predicted for the same bonded overlay. In every instance, identical slabs will undergo less load-related tensile stress when supported by a stiffer subgrade.

3. Loss of bond will lead to a significant decrease in pavement life. A 9-in. bonded overlay on the 20.0- × 20.0-ft slab with a modulus of subgrade reaction K = 200 pci will provide for more than 6,000 coverages. Without the bond, the number of allowable coverages drops to 267. The substantial loss in pavement life caused by the absence of bond between the overlay and the existing slab emphasizes how critical bond is to pavement performance.

Failure of almost all pavement sections will occur at the bottom of the existing slab where the tensile stresses are greatest. The exceptions are the slabs that have a 9-in. debonded overlay; in that case the overlay will have higher tensile stress than the thinner underlying slab. It is evident from this examination that one of the most important parameters in determining the life of pavement and overlay is the quality of the bond.

The effect of debonding on deflection was also investigated. Maximum pavement deflection occurs when the load is applied to the corner of the slab. A summary of the maximum deflection results of the ILLI-SLAB model is given in Table 3. Figures 8-10 show the deflection data in graphic form. Stiffer subgrades will reduce deflection by a substantial amount—as much as 49 percent. Figure 8 shows the resulting deflections

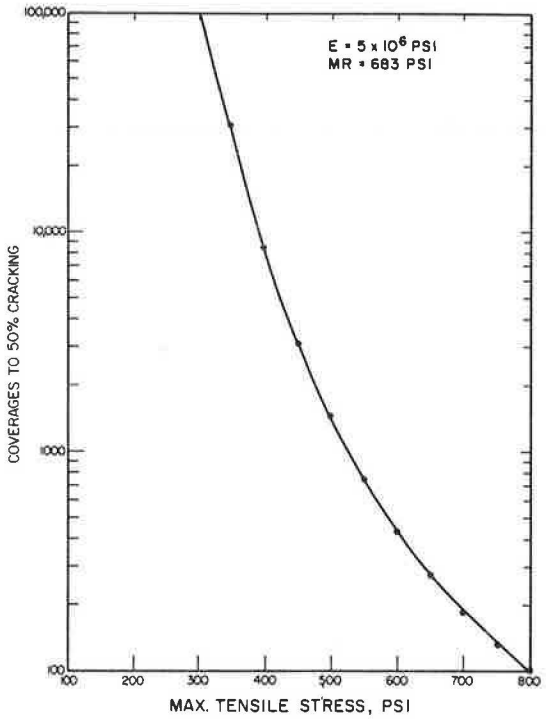

FIGURE 7 Effect of slab stresses on pavement life (coverages to 50 percent cracking).

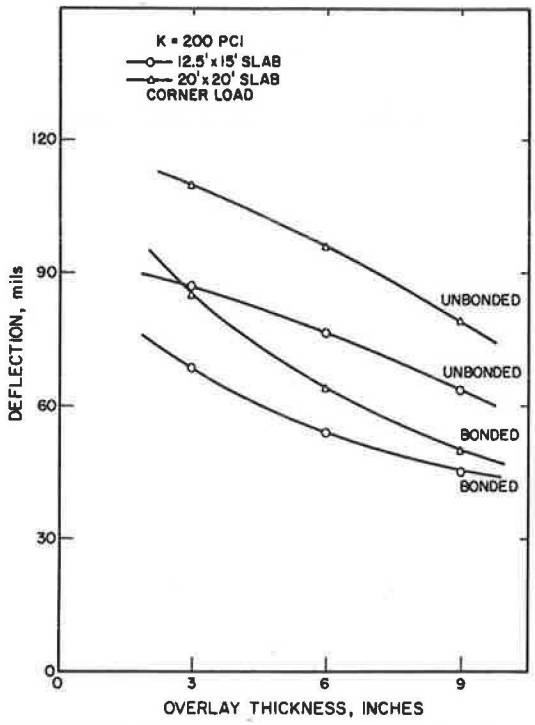

FIGURE 8 Maximum pavement deflection for varying overlay thicknesses in bonded and unbonded slabs with subgrade K = 200 pci.

TABLE 3 MAXIMUM CORNER DEFLECTIONS CALCULATED FOR CORNER LOADING

Slab Size (ft)	Overlay Thickness (in.)	K (pci)	Overlay Bond	Deflection (mils)
12.5 × 15.0	3	200	Bonded	68.8
12.5 × 15.0	6	200	Bonded	54.2
12.5 × 15.0	9	200	Bonded	45.5
12.5 × 15.0	3	500	Bonded	35.7
12.5 × 15.0	6	500	Bonded	28.8
12.5 × 15.0	9	500	Bonded	23.8
12.5 × 15.0	3	200	Unbonded	86.8
12.5 × 15.0	6	200	Unbonded	76.3
12.5 × 15.0	9	200	Unbonded	63.6
12.5 × 15.0	3	500	Unbonded	44.3
12.5 × 15.0	6	500	Unbonded	40.4
12.5 × 15.0	9	500	Unbonded	34.0
20.0 × 20.0	3	200	Bonded	85.9
20.0 × 20.0	6	200	Bonded	63.8
20.0 × 20.0	9	200	Bonded	50.4
20.0 × 20.0	3	500	Bonded	45.6
20.0 × 20.0	6	500	Bonded	36.0
20.0 × 20.0	9	500	Bonded	28.7
20.0 × 20.0	3	200	Unbonded	110.6
20.0 × 20.0	6	200	Unbonded	96.3
20.0 × 20.0	9	200	Unbonded	78.6
20.0 × 20.0	3	500	Unbonded	57.7
20.0 × 20.0	6	500	Unbonded	52.2
20.0 × 20.0	9	500	Unbonded	43.4

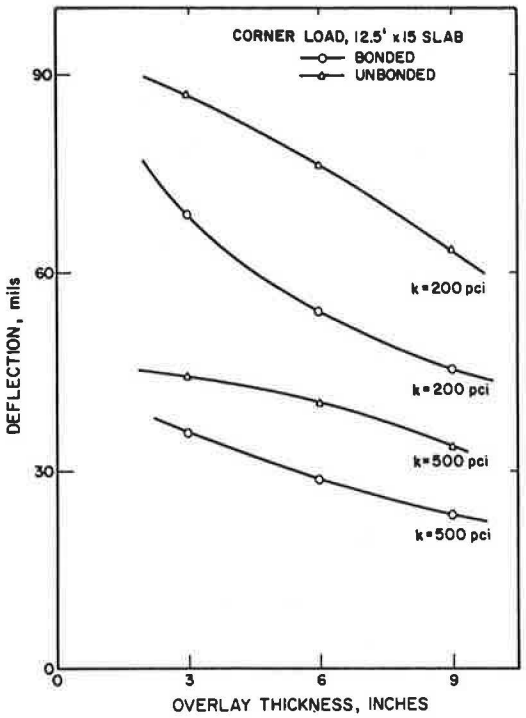

FIGURE 9 Maximum pavement deflection for varying overlay thicknesses in bonded and unbonded 12.5- × 15.0-ft slabs.

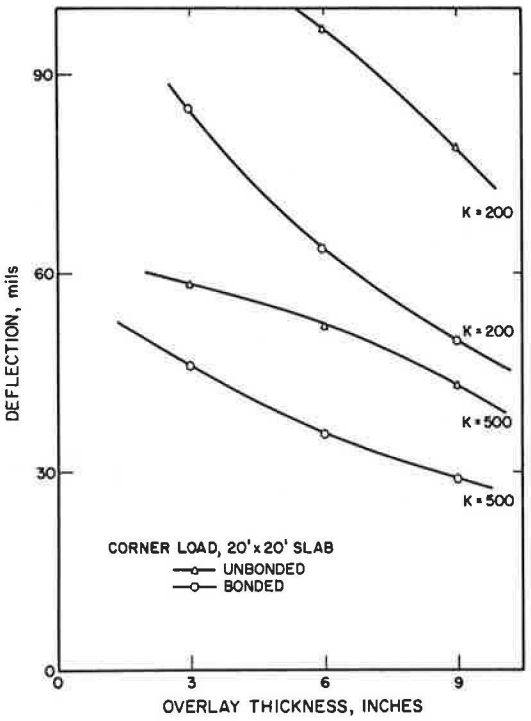

FIGURE 10 Maximum pavement deflection for varying overlay thicknesses in bonded and unbonded 20.0- × 20.0-ft slabs.

for two slab sizes. A larger slab is subjected to higher deflections if all other factors are held constant.

More important to this study is how maximum pavement deflection is influenced by the bond between the overlay and the existing slab. As can be seen in Figures 9 and 10, when all other factors are held constant, there is a large difference in corner deflections between the bonded and unbonded sections. Table 4 gives the percentage difference in deflection between bonded and unbonded sections. These differences vary from 19.4 to 35.9 percent with larger differences associated with thicker overlays. This finding is of great significance to the detection of debonding, as will be discussed later.

Curling Stresses

Temperature differentials that occur in the slab produce other stresses in the pavement. Depending on the climatic conditions, these stresses, known as curling stresses, can be extremely high. The Westergaard-Bradbury equations were used to predict the magnitude of the stresses, which developed at the interior and edge of a slab, caused by the slab's resistance to curling. In the analysis, a temperature gradient of 3°F/in. was used and values were calculated for 12.5- × 15.0-ft and 20.0- × 20.0-ft slabs 11, 14, and 17 in. thick. These thicknesses correspond to 3-, 6-, and 9-in. fully bonded overlays on an 8-in. slab. Two modulus of subgrade reaction values were examined, 200 and 500 pci. The results of this analysis are given in Table 5.

The effects of the combined load- and temperature-induced stresses on pavement design and performance were not the primary objective of this study, but this condition is extremely important in the evaluation of the effect of bond loss on the performance of bonded overlays. When the stress due to load is added to the edge-curling stress, extremely high stress levels are obtained. Table 6 gives the total tensile stress found when the stresses due to edge loading and temperature curling are added. The bonded condition is easily evaluated because it can be treated as a monolithic slab and all of the tensile stresses occur in the bottom of the slab. The Westergaard-Bradbury equations for layered systems are applicable to the bonded condition. However, the equations are not directly applicable to the unbonded condition because it consists of two separate layers.

The temperature gradient across the slab is not linear; it undergoes the greatest change in the top 4 in. of the pavement surface (Figure 11) (*14*). Therefore the highest temperature gradient will be located in the overlay, not in the underlying slab. It is believed that this condition can lead to the separation of the overlay from the original pavement when the temperature gradient is high and bond is absent. If a positive temperature gradient exists in the slab (the pavement surface is hotter than the bottom) and the overlay separates from the underlying slab, the weight of the overlay is supported by its corners and edges. If an interior load is then applied, large tensile stresses occur in the bottom of the overlay near the corners. If the temperature gradient is negative (i.e., warmer on the bottom than the top), the corners have a tendency to curl up off the underlying support. A corner load applied to the nonsupported area causes extremely high stresses in the top of the overlay.

TABLE 4 DEFLECTION DIFFERENCE BETWEEN SLABS WITH BONDED AND UNBONDED OVERLAYS

Slab Size (ft)	Overlay Thickness (in.)	K (pci)	Deflection (mils)		Percentage Difference
			Bonded	Unbonded	
12.5 × 15.0	3	200	68.8	86.8	20.7
12.5 × 15.0	6	200	54.2	76.3	29.0
12.5 × 15.0	9	200	45.5	63.6	28.5
12.5 × 15.0	3	500	35.7	44.3	19.4
12.5 × 15.0	6	500	28.8	40.4	28.7
12.5 × 15.0	9	500	23.8	34.0	30.0
20.0 × 20.0	3	200	84.9	110.6	23.2
20.0 × 20.0	6	200	63.8	96.3	33.8
20.0 × 20.0	9	200	50.4	78.6	35.9
20.0 × 20.0	3	500	45.6	57.7	21.0
20.0 × 20.0	6	500	36.0	52.2	31.0
20.0 × 20.0	9	500	28.7	43.4	33.9

TABLE 5 COMPARISON OF EDGE AND INTERIOR STRESSES FOR BONDED SLABS

Slab Size (ft)	Total Slab Thickness (in.)	K (pci)	Edge Stress (psi)	Interior Stress (psi)
12.5 × 15.0	11	200	247.5	276.6
12.5 × 15.0	14	200	220.5	236.8
12.5 × 15.0	17	200	108.4	189.1
12.5 × 15.0	11	500	342.4	392.0
12.5 × 15.0	14	500	351.8	396.1
12.5 × 15.0	17	500	331.5	362.6
20.0 × 20.0	11	200	305.2	461.0
20.0 × 20.0	14	200	372.8	494.1
20.0 × 20.0	17	200	357.0	502.5
20.0 × 20.0	11	500	412.5	485.3
20.0 × 20.0	14	500	472.5	555.9
20.0 × 20.0	17	500	497.2	585.0

TABLE 6 TOTAL TENSILE STRESS FROM LOAD AND TEMPERATURE IN SLABS WITH BONDED OVERLAYS

Slab Size (ft)	Total Slab Thickness (in.)	Subgrade K (pci)	Tensile Stress (psi)		
			ILLI-SLAB	Westergaard Curling	Total
12.5 × 15.0	11	200	787	248	1,035
12.5 × 15.0	14	200	547	220	767
12.5 × 15.0	17	200	401	108	509
12.5 × 15.0	11	500	641	342	983
12.5 × 15.0	14	500	466	352	818
12.5 × 15.0	17	500	350	332	682
20.0 × 20.0	11	200	788	305	1,093
20.0 × 20.0	14	200	588	373	961
20.0 × 20.0	17	200	416	357	773
20.0 × 20.0	11	500	638	412	1,050
20.0 × 20.0	14	500	465	472	937
20.0 × 20.0	17	500	357	497	854

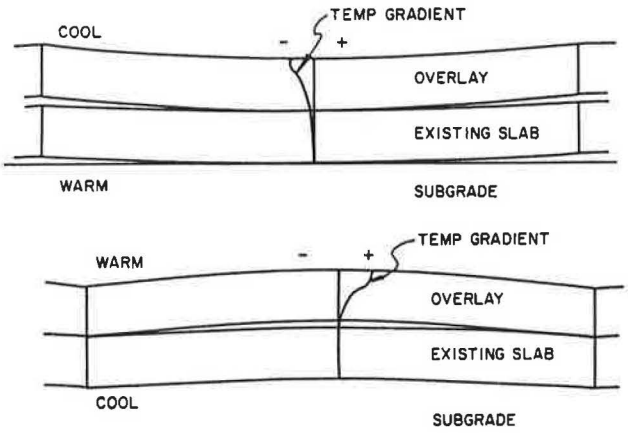

FIGURE 11 Slab separation caused by differential curling of unbonded slabs.

The phenomenon of differential slab curling in unbonded overlays was investigated by Lall and Lees (*15*). It was found that, when the corners of the overlay curl up off the underlying layer, the load-stress relation indicates that the slab undergoes three distinct phases as the incremental load is applied: (a) free bending, (b) support of the overlay by the underlying layer increasing from zero to full, and (c) full support of the overlay. Under these conditions, the critical stress will always occur in the overlay, not in the underlying slab.

The first attempt to determine the total tensile stresses that occur in debonded overlays used the calculated ILLI-SLAB stresses and the Westergaard-Bradbury equation for slabs 3, 6, and 9 in. thick on a very stiff subgrade (K = 10,000 pci). The results of the Westergaard-Bradbury analysis are given in Table 7. Because the Westergaard-Bradbury equations can only be used for one-layer systems, the use of a very stiff subgrade was an attempt at modeling the existing slab. For this analysis to be valid, the slabs would have to remain completely in contact with the underlying slab so that full support could be maintained. As mentioned, the overlay and existing slab may curl differentially as shown in Figure 11. Also, it is unlikely that the Westergaard-Bradbury equations were ever intended for use with such a high subgrade stiffness, which casts doubt on the validity of the results. The curling stress for each overlay was added to the load-induced tensile stress in each overlay calculated using ILLI-SLAB. Table 7 gives the total maximum tensile stress in the overlay found using this method. It is noted that these total maximum tensile stresses increase as the overlay becomes thicker. Because of the assumption that constant support is maintained and the limitations of the Westergaard-Bradbury equations, it is thought that this approach does not accurately represent actual pavement response.

A second approach was used in an effort to determine the total maximum tensile stress that occurs in an unbonded overlay that curls off the underlying slab. ILLI-SLAB was used to model two 12.5- × 15.0-ft overlaid slabs that contained areas of nonsupport (Figure 1). The wheel loads were placed over the nonsupported areas, and the resulting stresses are given in Table 8. These stresses are due only to the applied load. ILLI-SLAB considers the self-weight of the slab to be equal to zero, thus producing no stress in the slab due to its own weight. ILLI-SLAB does, however, incorporate the increased load-related stress levels produced when the overlay is not supported by the underlying slab.

It is admitted that the stresses that appear in Table 8 are unrealistically high because of the inability of the present ILLI-SLAB model to add support when the curled overlay comes into contact with the underlying slab. It is noted that any separation between the two slabs would be quite small, and they would readily come into contact if load were applied. Thus the high calculated stresses are not a true representation of field response.

There is, nevertheless, value in the data. The first point to be made is that the magnitude of the stress is many times greater for the thinner overlays than for the thicker overlays. The 3-in. overlay for the corner loading condition had 10 times the stress of that found for the 9-in. overlay. It must be realized that the 3-in. overlay will also have a greater

TABLE 7 TOTAL TENSILE STRESS IN UNBONDED OVERLAYS FROM LOAD AND TEMPERATURE

Slab Size (ft)	Overlay Thickness (in.)	Subgrade K (pci)	Tensile Stress (psi)		
			ILLI-SLAB	Westergaard Curling[a]	Total
12.5 × 15.0	3	200	428	116	544
12.5 × 15.0	6	200	668	232	900
12.5 × 15.0	9	200	652	348	1,000
12.5 × 15.0	3	500	338	116	454
12.5 × 15.0	6	500	538	232	770
12.5 × 15.0	9	500	536	348	884
20.0 × 20.0	3	200	426	116	542
20.0 × 20.0	6	200	665	232	897
20.0 × 20.0	9	200	654	348	1,002
20.0 × 20.0	3	500	337	116	453
20.0 × 20.0	6	500	536	232	768
20.0 × 20.0	9	500	538	348	886

[a]Westergaard calculations for unbonded overlays made using K = 10,000 psi (assumed stiffness of underlying slab).

TABLE 8 MAXIMUM TENSILE STRESS IN NONSUPPORTED UNBONDED OVERLAYS

Overlay Thickness (in.)	Load Position	Maximum Overlay Stress (psi)	Slab Deflection (in.)
3	Corner	16,278	2.50
6	Corner	3,292	0.82
9	Corner	1,628	0.48
3	Interior	2,332	0.14
6	Interior	1,271	0.08
9	Interior	802	0.05

tendency to curl off its support because (a) its average temperature gradient will be higher than that of the thicker overlays because the largest change in temperature occurs in the top 4 in. of the pavement surface and (b) it has less self-weight to prevent it from curling than do the thicker overlays. Thus a thinner overlay is much more likely to curl off its support than is a thicker overlay, and when loaded the thinner nonsupported overlay will experience greater stress than a thicker nonsupported overlay.

A second point to be made is that the stresses determined for the interior condition were much less than those found for the corner condition. These two findings agree with data obtained from field surveys in which debonding of bonded overlays results in characteristic corner and edge cracking of the overlay. This problem is far more prevalent in thin bonded overlays, possibly because the overlay has curled up off the underlying surface. Maximum tensile stress always occurs at the bottom of the underlying slab for thin overlays if the two layers remain in contact. Only when the two layers separate because of curling will the maximum tensile stress occur in the overlay. This evidence suggests that it is critical that a strong bond be established at all parts of the slab, particularly at the edges and corners.

ACHIEVING BOND

Obtaining a good bond between the overlay and the existing pavement section is crucial to the successful performance of the overlay. Much has been written about proper construction techniques for bonded concrete overlays. The following is a brief summary of some important aspects of achieving a good bond.

The most important factor in obtaining a successful bond is preparation of the existing surface before placement of the overlay. According to Bergren (*4*), "The most critical factor that affects bond . . . is that the surface must be extremely clean and dry prior to the placement of the grout and subsequent placement of the concrete resurfacing." Common surface-cleaning techniques use high-pressure water, sandblasting, or metal shot to remove surface contaminants. When the unsound concrete and surface contaminants have been removed from the existing pavement (and it has been allowed to dry if water cleaning was used), a bonding medium must be applied. Bonding media such as sand-cement grouts, neat cements, or commercially available epoxies and latex cements have been used successfully. It is important that the bonding agent not be allowed to dry before placement of the resurfacing material, otherwise a good bond cannot be obtained.

Research has shown that when bond has been established it will remain. Gillette (*1*) stated that "wherever loss of bond occurs, it probably developed soon after construction; little or no growth in the loss of bond area occurs over a period of time and under traffic." Thus when bond loss occurs it is due to conditions present during or shortly after construction. The primary cause of bond loss is to be found in the preparation of the existing pavement surface. Inadequate removal of unsound concrete or tire rubber, paint strips, and oil could prevent the bond from developing. A wet pavement surface, a thick layer of grout, or thin and watery grout could also contribute to bond loss. When bond is lost, characteristic distress occurs in the resurfacing, such as edge and corner breaks caused when the delaminated areas are subjected to load. Starting as hairline cracks, the distress eventually spalls and ravels and may result in displacement of the broken overlay.

DETECTING DEBONDING

Present practices rely on "sounding" of the pavement surface or coring to determine if debonding has occurred. Sounding of the pavement can be done manually by dropping a steel rod onto the surface or striking it with a hammer. A delaminated overlay will resound with a thud, and a bonded pavement will ring. There is also automated equipment that is based on this principle. Cores from an overlaid section can be visually and physically examined to determine if debonding has occurred. Both of these procedures are time consuming and expensive and are not normally done during routine pavement evaluation.

The results of the ILLI-SLAB analysis indicate that debonded sections have significantly higher corner deflections under load than do bonded sections, even without differential curling. Therefore it is theoretically possible to find debonding between the overlay and the existing slab by comparing the corner deflections produced through nondestructive testing (NDT) with those calculated using a finite-element model. Significantly higher NDT corner deflections would indicate that a problem in the pavement structure may exist and that one of the possible causes could be loss of bond between the

layers. Further examination of the distressed locations, possibly a limited coring program, could then be used to positively identify the causes of the higher deflection.

There are some problems that may possibly be encountered with this proposed procedure. The first can be attributed to NDT itself. Great variation in deflections can occur because of changes in weather or seasonal changes. The NDT program must be well planned, and such factors must be taken into account when deflections are calculated. Second, it would probably be common for slabs to contain both bonded and debonded areas. At the present time, ILLI-SLAB cannot model this condition; thus how partial bonding influences corner deflection is not known. Further investigation and field verification are necessary to prove the proposed method.

CONCLUSION

This study has shown that portland cement concrete slabs composed of an existing slab and a bonded overlay respond to load and curling forces differently than does an existing slab with an unbonded overlay. The absence of bond destroys the monolithic structure of the pavement section, detrimentally affecting the maximum pavement tensile stress and deflection due to load. Curling stresses are a major factor in the total maximum tensile stress in the pavement section, but they are not easily determined for the unbonded condition. The following conclusions are drawn from this study:

1. Maximum pavement tensile stress and deflection due to load decrease as subgrade becomes stiffer for both the bonded and the debonded overlay condition.
2. For the two slab sizes studied, maximum tensile stress due to load is relatively unaffected by slab size whereas maximum deflection increases as slab size increases.
3. The existence of a good bond between the overlay and the existing slab greatly reduces maximum tensile stress and corner deflections due to load.
4. An unbonded overlay may separate from the underlying slab because of a high temperature gradient across the overlay, the relatively low self-weight of the overlay, and the extremely stiff supporting layer.
5. Thinner unbonded overlays are more likely to separate from the underlying slab and will suffer higher maximum tensile stresses due to load than do thicker overlays.
6. Good construction practices must be used to guarantee that a good bond forms between the overlay and the existing pavement.
7. It may be possible to use NDT corner deflections to determine if debonding of the overlay has occurred.

REFERENCES

1. R. W. Gillette. A 10-Year Report on Performance of Bonded Concrete Resurfacings. In *Highway Research Record 94*, HRB, National Research Council, Washington, D.C., 1965, pp. 61-76.
2. M. I. Darter and E. J. Barenberg. *Bonded Concrete Overlays: Construction and Performance.* Paper GL-80-11. U.S. Army Engineer Waterways Experiment Station, Vicksburg, Miss., Sept. 1980.
3. E. J. Felt. Resurfacing and Patching Concrete Pavements with Bonded Concrete. *HRB Proc.*, Vol. 35, 1956, pp. 444-469.
4. J. V. Bergren. Bonded Portland Cement Concrete Resurfacing. In *Transportation Research Record 814*, TRB, National Research Council, Washington, D.C., 1981, pp. 66-70.
5. *Resurfacing with Portland Cement Concrete.* NCHRP Project 99. TRB, National Research Council, Washington, D.C., Dec. 1982.
6. M. R. Thompson, E. J. Barenberg, A. M. Ioannides, and J. A. Fischer. *Development of a Stress-Dependent Finite Element Slab Model.* Department of Civil Engineering, University of Illinois, Urbana, 1983.
7. L. W. Teller and E. C. Sutherland. The Structural Design of Concrete Pavements, Part 2: Observed Effects of Variations in Temperature and Moisture on the Size, Shape, and Stress Resistance of Concrete Pavement Slabs. *Public Roads*, Vol. 16, No. 9, 1935.
8. M. I. Darter. *Design of Zero-Maintenance Plain Jointed Concrete Pavement*, Vol. I: *Development of Design Procedure.* FHWA Report FHWA-RD-77-111. FHWA, U.S. Department of Transportation, June 1977.
9. E. J. Yoder and M. W. Witczak. *Principles of Pavement Design*, 2d ed. Wiley-Interscience, New York, 1975.
10. H. M. Westergaard. Analysis of Stresses in Concrete Pavements Due to Variations in Temperature. *HRB Proc.*, Vol. 6, 1926, pp. 201-217.
11. R. D. Bradbury. *Reinforced Concrete Pavements.* Wire Reinforcement Institute, Washington, D.C., 1938.
12. ERES Consultants. *Non-Destructive Structural Evaluation of Airfield Pavements.* U.S. Army Engineer Waterways Experiment Station, Vicksburg, Miss., Dec. 1982.
13. *Airport Pavement Design and Evaluation.* Advisory Circular 150/5320-6C. FAA, U.S. Department of Transportation, Dec. 7, 1978.
14. B. J. Dempsey. *A Heat-Transfer Model for Evaluating Frost Action and Temperature Related Effects in Multilayered Pavement Systems.* Ph.D. dissertation. University of Illinois, Urbana, 1969.
15. B. Lall and G. Lees. Analysis of Stresses in Unbonded Concrete Overlay. In *Transportation Research Record 930*, TRB, National Research Council, Washington, D.C., 1983, pp. 25-31.

The views of the authors do not purport to reflect the position of the Department of the Army or the Department of Defense.

DISCUSSION

GEORGE T. KOROVESIS AND ANASTASIOS M. IOANNIDES
University of Illinois, Urbana, Ill. 61801.

The authors have undoubtedly presented a valuable piece of work—an attempt to determine the effect of debonding of concrete overlays on pavement response. As they point out, when it comes to the calculation of curling stresses in a slab resting on a dense liquid (Winkler) subgrade, the only analytical model available is that proposed by Westergaard. He suggested that "stresses due to variations of temperature

are to be combined with the stresses due to the loads" and that "this combination, in most cases, is a simple matter of addition" (*1*). Since the 1920s superposition has been the conventional way of investigating this combined effect [see, for example, Bradbury (*2*)], although as early as 50 years ago Teller and Sutherland (*3*) provided experimental data indicating the shortcomings of this approach. The authors have also used it to obtain the total stress, by summing the stress due to the load alone plus the stress due to the temperature differential alone.

The validity of the superposition approach depends on whether the following two basic conditions are met in the calculation of both of the individual stress components:

- Small deformations and
- Same boundary conditions.

Even if it is accepted that the deformations are indeed small in the two cases, it cannot usually be accepted that the boundary conditions are the same. If a flat slab is loaded, practically all points on its bottom surface are in contact with the subgrade (except, perhaps, for a few points far away from the load). However, under curling conditions, a large portion of the slab may lose contact with the subgrade, depending on the temperature differential and the radius of relative stiffness. If load is then placed on an unsupported area, superposition will not apply.

Results from ILLI-SLAB given in Table 9 illustrate this assertion. They were obtained using a new subroutine recently implemented in ILLI-SLAB to calculate stresses due to curling and external loads, combined or individually, and account for the presence of gaps underneath the slab and for loss of support. The finite-element model employed is the one proposed by Huang and Wang (*4*) and Chou (*5*). Through an iterative procedure, this formulation also accommodates the regaining of subgrade support.

The limited amount of data given in Table 9 indicates that edge loading generally remains critical with respect to stresses, especially under a positive (daytime) temperature differential. Under a high negative (nighttime) gradient, a slab resting on a stiff subgrade may develop a higher combined stress under corner loading. The total stress computed by superposition underestimates the corresponding one from ILLI-SLAB in the cases of interior and edge loading when the slab is under a positive gradient, particularly when the temperature differential is large and the subgrade is stiff. On the other hand, superposition will lead to a conservative estimate of the combined stress during nighttime conditions, as well as under corner loading during the day especially for soft subgrades and a large positive differential. It is therefore observed that superposition and ILLI-SLAB agree only when the two previously mentioned conditions are satisfied (i.e., when a low gradient is applied on a slab resting on a soft subgrade).

Note that, in practice, the wisdom of relying on curling stresses to relieve part of the stress induced by external loads is debatable. Fortunately, given that for interior and edge loading this will occur only under nighttime conditions, the decision to allow for such stress relief is largely inconsequential as far as the fatigue life of the pavement is concerned.

Westergaard's theory (*1*), in the form of the Bradbury (*2*) coefficient (C), has been used by the authors to obtain curling stresses. This theory is also based on certain assumptions and should not be used indiscriminately. The two basic assumptions are

- Infinite and weightless slab and
- Full contact between slab and subgrade.

Other pertinent assumptions may be found elsewhere (*6*).

The data in Table 10 indicate that, for relatively large slabs resting on a soft subgrade and under a small temperature differential, there is good agreement between ILLI-SLAB results and Westergaard theory. When the basic assumptions are not fulfilled, a finite-element program like ILLI-SLAB, which can take into account the self-weight of the slab and the loss of subgrade support, should be used instead of the Westergaard theory. ILLI-SLAB results in Table 10 indicate that the case of a negative temperature differential is not merely a mirror image of the corresponding positive gradient condition, as suggested by Westergaard and Bradbury. Under a positive gradient a short slab resting on a stiff

TABLE 9 COMPARISON OF SUPERPOSITION AND ILLI-SLAB RESULTS

K (psi)	ΔT (°F)	Interior Load				Stress Under Edge Load (psi)				Corner Load			
		L	C	TS	TI	L	C	TS	TI	L	C	TS	TI
200	-21	384	-64	320	293	658	-26	632	579	-482	-54	-536	-413
200	-42	384	-83	301	241	658	-32	626	511	-482	-62	-544	-418
200	+21	384	70	454	484	658	40	698	753	-482	72	-410	-378
200	+42	384	89	473	585	658	55	713	839	-482	97	-385	-332
500	-21	329	-84	245	212	579	-33	546	456	-415	-69	-484	-435
500	-42	329	-101	228	163	579	-36	543	387	-415	-77	-492	-449
500	+21	329	88	417	509	579	59	638	744	-415	92	-323	-330
500	+42	329	105	434	661	579	72	651	880	-415	113	-302	-268

NOTE: Slab is 12.5 × 15.0 ft; E = 5 million psi, μ = 0.15, h = 14 in.; $\varepsilon_t = 5 \times 10^{-6}$ in./in./°F; load = B-727 (two loads 12 × 20 in. at 268 psi); L = stress due to external load; C = curling stress due to temperature differential; TS = total stress (superposition); TI = total stress (ILLI-SLAB). All stresses are tensile and are positive when at the bottom of the slab and negative when at the top. For each loading condition, all stresses act at the same location.

TABLE 10 COMPARISON OF BRADBURY AND ILLI-SLAB CURLING STRESSES

				Stress at Interior (psi)					
				δT = +1.5°F/in.			δT = -3.0°F/in.		
K (pci)	h (in.)	Lx/l	Ly/l	IS	B	Percentage	IS	B	Percentage
50	8	4.16	3.33	64	61	105	-103	-121	85
50	8	5.55	3.33	107	106	101	-183	-212	86
50	10	3.52	2.82	50	48	104	-80	-99	81
50	10	4.70	2.82	100	98	102	-160	-194	82
50	10	5.87	2.82	138	138	100	-239	-277	86
50	10	7.05	2.82	159	161	99	-297	-323	92
50	14	2.74	2.19	30	28	107	-51	-60	85
50	14	3.65	2.19	75	71	106	-115	-133	86
500	8	7.40	5.92	119[a]	145	82	-187	-291	64
500	8	9.87	5.92	146	148	99	-262	-295	89
500	10	6.26	5.01	113[a]	162	70	-155	-325	48
500	10	8.35	5.01	159[a]	182	87	-254	-365	70
500	10	10.44	5.01	176	179	98	-320	-358	89
500	10	12.53	5.01	177	176	101	-339	-352	96
500	14	4.87	3.89	91[a]	159	57	-110	-317	35
500	14	6.49	3.89	165[a]	221	75	-197	-442	45

NOTE: Slab length = 15 to 30 ft; slab width = 12 ft; E = 4 million psi; μ = 0.15; $\epsilon_t = 5 \times 10^{-6}$ in./in./°F; IS = ILLI-SLAB; B = Bradbury (interior); Percentage = (IS/B) × 100%. All stresses are tensile and positive when at the botton of the slab and negative when at the top.
[a]A higher stress occurs at the edge.

subgrade may experience a maximum curling stress at its edge rather than at the interior.

The theoretical curling stress will underestimate ILLI-SLAB's prediction when a short slab is under a positive temperature differential and the subgrade is soft. The reverse is true when a short slab rests on a stiff subgrade or is under a negative gradient. Slab length is thus a more important parameter when the temperature differential is considered than it is under an external load alone. The slab size ratio (L/l), of the slab length to the radius of relative stiffness, required for the development of the infinite-slab bending stress under an external load, was found to be only about 5.0 (*7*). A value closer to 10.0 is indicated by the curves in Figure 12 [i.e., slab size remains influential even with much larger slabs (*2*)]. Longer slabs under the same temperature differential are subject to more bending action because a greater part of the slab loses contact with the subgrade.

Note that a stiffer subgrade does not always mean lower stresses in the slab or a longer life expectancy for the pavement when combined stresses are considered. Examples of this are given in Tables 9 and 10, in which curling stresses are higher for stiffer subgrades, as both ILLI-SLAB and the Westergaard-Bradbury theory indicate. This effect becomes more pronounced for shorter slabs under lower gradients.

It should be pointed out that there is appreciable difference between the curve for the coefficient C given by Bradbury (*2*, Figure 2) and that given by Yoder and Witczak (*8*, Figure 3.4). The original by Bradbury, which also agrees with Westergaard's data (*1*), is probably a better choice and was used in deriving the results in Table 10. Both curves are reproduced in Figure 12.

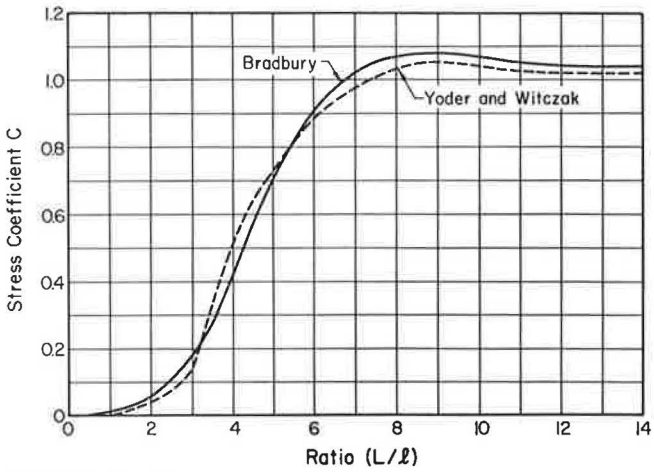

FIGURE 12 Chart for curling stress coefficient (C).

REFERENCES

1. H. M. Westergaard. Analysis of Stresses in Concrete Pavements Due to Variations of Temperature. *HRB Proc.*, Vol. 6, 1926, pp. 201-217.
2. R. D. Bradbury. *Reinforced Concrete Pavements.* Wire Reinforcement Institute, Washington, D.C., 1938.
3. L. W. Teller and E. C. Sutherland. The Structural Design of Concrete Pavements, Part 2: Observed Effects of Variations in Temperature and Moisture on the Size, Shape, and Stress Resistance of Concrete Pavement Slabs. *Public Roads*, Vol. 16, No. 9, 1935.
4. Y. H. Huang and S. T. Wang. Finite-Element Analysis of Rigid Pavements with Partial Subgrade Contact. In *Transportation Research Record 485*, TRB, National Research Council, Washington, D.C., 1974, pp. 39-54.

5. Y. T. Chou. *Structural Analysis Computer Programs for Rigid Multicomponent Pavement Structures with Discontinuities—WESLIQID and WESLAYER*. Reports 1-3, Technical Report GL-81-6. U.S. Army Engineer Waterways Experiment Station, Vicksburg, Miss., May 1981.
6. H. M. Westergaard. Stresses in Concrete Pavements Computed by Theoretical Analysis. *Public Roads*, Vol. 7, No. 2, April 1926. (Also in *HRB Proc.*, Vol. 5, Part I, 1926, pp. 90-112 as Computation of Stresses in Concrete Roads.)
7. A. M. Ioannides, M. R. Thompson, and E. J. Barenberg. Westergaard Solutions Reconsidered. In *Transportation Research Record 1043*, TRB, National Research Council, Washington, D.C., 1985, pp. 13-23.
8. E. J. Yoder and M. W. Witczak. *Principles of Pavement Design*, 2d ed. Wiley-Interscience, New York, 1975.

AUTHORS' CLOSURE

The authors appreciate the additional insights into debonded concrete overlay temperature- and load-induced stresses presented by Korovesis and Ioannides.

Publication of this paper sponsored by Committee on Pavement Rehabilitation.